ORIGINAL PAPER

NOVEL EXACT AND APPROXIMATE SOLUTIONS OF THE NEWELL-WHITEHEAD-SEGEL TYPE EQUATIONS

DERYA YILDIRIM SUCU[1], KHALİD KARAM ALİ[2],
SEYDİ BATTAL GAZİ KARAKOC[1]

Manuscript received: 04.01.2025; Accepted paper: 10.05.2025;
Published online: 30.06.2025.

Abstract. *The main goal of this study is to find different and new analytical and numerical solutions of the Newell-Whitehead-Segel-type equations, which belong to the most consequential amplitude equations in physical phenomena, such as fluid mechanics, solid-state physics, optics, plasma physics, dispersion, and chemical kinetics. To address the inherent complexities associated with the nonlinear equation, the researchers employed highly effective techniques: the novel* $(\frac{\varsigma'}{k\varsigma'+\varsigma+r})$ *-expansion method and the septic B-spline collocation method. The error norms* L_2 *and* L_∞ *are calculated for the adequacy and efficiency of the present method. The method's unconditional stability is demonstrated through the use of von-Neumann stability analysis. The appropriate solutions for the three test problems are found by computing the* L_2 *and* L_∞ *error norms, which highlight the significance of the procedure and demonstrate its applicability and credibility. The inferred numerical results show good agreement with the analytical solutions, indicating that the current B-spline collocation approach is a robust and attractive algorithm. The results are tabulated and reported both modally and in terms of the productivity of the procedure. The results produced from both analytical and numerical methods demonstrate the great utility of this study for scientists tasked with identifying characteristics and features of nonlinear processes across a variety of scientific domains.*

Keywords: *Newell-Whitehead-Segel equation;* $(\frac{\varsigma'}{k\varsigma'+\varsigma+r})$ *-expansion method; collocation; septic B-spline.*

1. INTRODUCTION

Non-equilibrium systems have mostly been observed in a variety of extended states, including pattern, chaotic, oscillatory, and uniform states, in nonlinear processes. Numerous striped patterns, like seashell stripes or sand ripples, occur across a range of spatially extended systems that can be represented by a system of equations known as amplitude equations. The theory of pattern creation heavily relies on amplitude equations. A fundamentally significant amplitude equation that describes how the stripe pattern appears in two-dimensional systems is the Newell-Whitehead-Segel (N-W-S) equation.

[1] Nevşehir Hacı Bektaş Veli University, Faculty of Sciences and Arts, Department of Mathematics, 50300 Nevşehir, Turkey. E-mail: dryldrmsucu@gmail.com; sbgkarakoc@nevsehir.edu.tr.
[2] Al-Azhar University, Faculty of Sciences, Department of Mathematics, Nasr-City, 4434104 Cairo, Egypt. E-mail: khalidkaram2012@azhar.edu.eg.

Once more, the equation has been performed as an effective mathematical scheme in different systems, such as Rayleigh–Bénard convection, Faraday instability, Taylor–Couette flow, directional solidification, biological systems, and chemical reaction [1,2]. The Newell–Whitehead (N-W) equation is written as [3]

$$u_t = au_{xx} + bu + -cu^3 = 0. \tag{1}$$

This equation has been modified by Segel and reformulated as follows [4]:

$$u_t = ku_{xx} + au - bu^q = 0, \qquad u(x,t) \in [A,B] \times [0,T] \tag{2}$$

where a, b, k, and q are positive integers. The N-W-S equation is widely applicable in biology, ecology, bioengineering, and mechanical and chemical engineering. It should be noted that Eq. (2) incorporates a number of well-known nonlinear equations from mathematical biology and physics. For example, if the equation becomes the heat equation with diffusivity constant k; if $a=0$, it becomes the non-linear diffusion equation, defining unstable heat conduction with a non-linear power-law source. Eq. (2), which has a response term of the type $au(1-u)$, simplifies to the well-known Fisher's equation when $q=2$ and $a=b$. With a reaction term of $au(1-u)$, Eq. (2) for $q=3$and $a=b$ becomes the Allen-Cahn equation [5,6]. It is a specific instance of the FitzHugh–Nagumo equation for $q=3$ and $a=b=-1$, which is found in the study of nerve cells [7,8]. The N-W equation, which is another important equation in this class, is altered by adding $q=3$ [3].

The N-W-S equation has been given crucial attention in recent years by presenting several methods and techniques, such as, differential transform method [1,9], Adomian decomposition method [10], homotopy perturbation method [11], finite difference scheme [12,13,14], cubic B-spline collocation method [15,16], sine–Gordon equation expansion method [17], He's variational iteration method [18], lattice Boltzmann scheme [19], $(G^{'}/G)$ expansion method [20], perturbation iteration transform method [21], variational iteration method [22,23], Deep Learning method [24], Elzaki Adomian decomposition [25,26]. Also in recent years, a variety of methods have been used to solve the Allen-Cahn equation, including a wavelet-based approximation method [27], a convergent finite difference scheme [28], a Haar wavelet method [29], a trigonometric B-spline collocation method [30], and so on. As is evident, these equations have been resolved in a number of ways, yet looking for more intriguing answers is still quite beneficial.

In this paper, we take notice of the well-known N-W-S equation, Eq. (2), with the following

$$u(A,t) = f_1(x) \text{ and } u(B,t) = f_2(x), \quad t \geq 0 \tag{3}$$

boundary conditions and

$$u(x,0) = g(x) \tag{4}$$

initial condition. This study paper is precise as follows: Section 2 of this work presents strategy and mathematical analysis of $(\frac{\varsigma'}{k\varsigma'+\varsigma+r})$-expansion method. In Section 3,

$(\frac{\varsigma'}{k\varsigma'+\varsigma+r})$-expansion method is used to obtain a new family of analytical solutions of the equation. Section 4 discusses the graphical representation of several of these solutions. Section 6 includes a stability analysis of the numerical scheme after Section 5 specifies septic B-spline functions and their characteristics, which are then applied to the equation. Then in Section 7, to show the performance and sensitivity of the method, the problem has been solved by taking different parameters, and the results are shown in tables. In Section 8, a brief presentation of the results is given.

2. THE STRATEGY OF THE ANALYTICAL TECHNIQUES

To obtain analytical localized solutions for the model (2), we consider a solution of the following form:

$$u(x,t) = U(\xi) \tag{5}$$

here, ξ

$$\xi = \eta x - \Omega t. \tag{6}$$

Upon substituting the provided representations (5) and (6) into Eq. (2), we obtain the following the nonlinear differential equation:

$$-aU(\xi) + bU(\xi)^q - \eta^2 k U''(\xi) - \Omega U'(\xi) = 0. \tag{7}$$

2.1. THE $(\frac{\varsigma'}{k\varsigma'+\varsigma+r})$ -EXPANSION METHOD

The $(\frac{\varsigma'}{k\varsigma'+\varsigma+r})$-expansion method [31,32] has radical steps presented in what follows:

Step 1. Presume the solution of (7) is given by:

$$U(\xi) = \sum_{i=0}^{N} M_i \Im(\xi)^i, \tag{8}$$

where $\Im(\xi) = (\frac{\varsigma'}{k\varsigma'+\varsigma+r})$, $\varsigma(\xi)$ provide the differential equation of the second-order:

$$\varsigma''(\xi) = -\frac{\wp}{\sigma}\varsigma'(\xi) - \frac{U}{\sigma^2}\varsigma(\xi) - \frac{U}{\sigma^2}r, \tag{9}$$

where: k, U, $\wp$, and σ are constants that will be chosen later, and M_i are unknown constants. The ODE's solution is $\Im = \Im(\xi)$;

$$\Im'(\xi) = (\wp - U - 1)\Im(\xi)^2 + \frac{1}{\sigma}(2U - \wp)\Im(\xi) - \frac{1}{\sigma^2}U. \tag{10}$$

Step 2. Applying the idea from the previous part to calculate *N*.

Step 3. We are able to solve (10) in two classes:

Class 1. When $H = \wp^2 - 4U > 0$,

$$\varsigma = -r + p_1 e^{\frac{1}{2\sigma}(-\wp - \sqrt{H})\xi} + p_2 e^{\frac{1}{2\sigma}(-\wp + \sqrt{H})\xi}, \tag{11}$$

p_1 and p_2 are arbitrary constants, must validate the relation $r^2 + p_1^2 + p_2^2 \neq 0$, then

$$\Im(\xi) = \frac{p_1(\wp + \sqrt{H}) + p_2(\wp - \sqrt{H})e^{\frac{\sqrt{H}\xi}{\sigma}}}{\sigma p_1(\wp - 2 + \sqrt{H}) + \sigma p_2(\wp - 2 - \sqrt{H})e^{\frac{\sqrt{H}\xi}{k}}}$$

$$\Im(\xi) = \tag{12}$$

$$\frac{[\wp(p_2 - p_1) - \sqrt{H}(p_2 + p_1)]\sinh(\frac{\sqrt{H}\xi}{2\sigma}) + [\wp(p_2 - p_1) - \sqrt{H}(p_2 - p_1)]\cosh(\frac{\sqrt{H}\xi}{2\sigma})}{\sigma[(\wp - 2)(p_2 - p_1) - \sqrt{H}(p_2 + p_1)\sinh(\frac{\sqrt{H}\xi}{2\sigma}) + \sigma[(\wp - 2)(p_2 + p_1) - \sqrt{H}(p_2 - p_1)]\cosh(\frac{\sqrt{H}\xi}{2\sigma})}$$

$$\Im(\xi) = \begin{cases} \dfrac{\wp - 2U}{2\sigma(\wp - U - 1)} - \dfrac{\sqrt{H}}{2\sigma(\wp - U - 1)}\tanh(\dfrac{\sqrt{H}\xi}{2\sigma}), & (\wp - 2)(p_2 - p_1) - \sqrt{H}(p_2 + p_1) = 0, \\ \dfrac{\wp - 2U}{2\sigma(\wp - U - 1)} - \dfrac{\sqrt{H}}{2\sigma(\wp - U - 1)}\coth(\dfrac{\sqrt{H}\xi}{2\sigma}), & (\wp - 2)(p_2 + p_1) - \sqrt{H}(p_2 - p_1) = 0. \end{cases} \tag{13}$$

Class 2. When $H = \wp^2 - 4U < 0$,

$$\varsigma = -r + e^{\frac{-\wp q}{2\sigma}}(p_1 \cos(\frac{\sqrt{-H}\xi}{2k}) + p_2 \sin(\frac{\sqrt{-H}\xi}{2\sigma}), \tag{14}$$

$$\Im(\xi) = \frac{(\wp p_1 - \sqrt{-H}p_2)\cos(\frac{\sqrt{-H}\xi}{2\sigma}) + (\wp p_2 + \sqrt{-H}p_1)\sin(\frac{\sqrt{-H}\xi}{2\sigma})}{\sigma((\wp - 2)p_1 - \sqrt{-H}p_2)\cos(\frac{\sqrt{-H}\xi}{2\sigma}) + \sigma((\wp - 2)p_2 + \sqrt{-H}p_1)\sin(\frac{\sqrt{-H}\xi}{2\sigma})} \tag{15}$$

$$\Im(\xi)=\begin{cases}\dfrac{\wp-2U}{2\sigma(\wp-U-1)}+\dfrac{\sqrt{-H}}{2\sigma(\wp-U-1)}\tan(\dfrac{\sqrt{-H}\,\xi}{2\sigma}), & (\wp-2)\,p_2+\sqrt{-H}\,p_1=0,\\ \dfrac{\wp-2U}{2\sigma(\wp-U-1)}-\dfrac{\sqrt{-H}}{2\sigma(\wp-U-1)}\cot(\dfrac{\sqrt{-H}\,\xi}{2\sigma}), & (\wp-2)\,p_1-\sqrt{-H}\,p_2=0.\end{cases} \tag{16}$$

Step 4. A system of equations appears when (8) and (10) are inserted into (7), since the coefficients with the same powers of $\Im(\xi)$ vanish.

3. APPLICATIONS

Now, to apply our methods for solving (7), we balance U^q with U'' to determine the value of N. Since $qN=N+2$, it leads to $N=\dfrac{2}{q-1}$, but N must be a positive integer. So, we take the transformation:

$$U(\xi)=V(\xi)^{1/q-1}. \tag{17}$$

Substituting from (17) into (7), we get the following equation:

$$-a(q-1)V(\xi)^2+b(q-1)V(\xi)^3+\frac{\eta^2k(q-2)V'^2}{q-1}-\eta^2kV(\xi)V''(\xi)-\Omega V(\xi)V'(\xi)=0. \tag{18}$$

By making the balancing again between V^3 and VV'', we obtain $N=2$.

3.1. THE $\left(\dfrac{\varsigma'}{k\varsigma'+\varsigma+r}\right)$ *EXPANSION METHOD*

Solution of (18) based on (8) is:

$$V(\xi)=M_0+M_1\Im(\xi)+M_2\Im^2(\xi). \tag{19}$$

We enter (19) into (18) and set the coefficients of $\Im(\xi)$ to zero with equal power to arrive at the system below:

$$-aM_0^2q+aM_0^2+bM_0^3q-bM_0^3-\frac{\eta^2k\wp UM_1M_0}{\sigma^3}-\frac{2\eta^2kU^2M_2M_0}{\sigma^4}+\frac{2\eta^2kU^2M_1M_0}{\sigma^3}$$
$$+\frac{\eta^2kU^2M_1^2q}{(q-1)\sigma^4}-\frac{2\eta^2kU^2M_1^2}{(q-1)\sigma^4}+\frac{UM_1M_0\Omega}{\sigma^2}=0,$$

$$-2aM_0M_1q+2aM_0M_1+3bM_0^2M_1q-3bM_0^2M_1-\frac{\eta^2k\wp^2M_0M_1}{\sigma^2}-\frac{\eta^2k\wp UM_1^2}{\sigma^3}$$
$$-\frac{6\eta^2k\wp UM_0M_2}{\sigma^3}+\frac{6\eta^2k\wp UM_0M_1}{\sigma^2}-\frac{2\eta^2kU^2M_1M_2}{\sigma^4}+\frac{2\eta^2kU^2M_1^2}{\sigma^3}+\frac{12\eta^2kU^2M_0M_2}{\sigma^3}$$
$$-\frac{6\eta^2kU^2M_0M_1}{\sigma^2}-\frac{2\eta^2kUM_0M_1}{\sigma^2}+\frac{2\eta^2k\wp UM_1^2q}{(q-1)\sigma^3}-\frac{4\eta^2k\wp UM_1^2}{(q-1)\sigma^3}+\frac{4\eta^2kU^2M_1M_2q}{(q-1)\sigma^4}$$
$$-\frac{8\eta^2kU^2M_1M_2}{(q-1)\sigma^4}+\frac{8\eta^2kU^2M_1^2}{(q-1)\sigma^3}-\frac{4\eta^2kU^2M_1^2q}{(q-1)\sigma^3}+\frac{\wp M_0M_1\Omega}{\sigma}+\frac{UM_1^2\Omega}{\sigma^2}$$
$$+\frac{2UM_0M_2\Omega}{\sigma^2}-\frac{2UM_0M_1\Omega}{\sigma}=0,$$
$$\frac{6k\wp UM_1^2\eta^2}{\sigma^2}+\frac{kq\wp^2M_1^2\eta^2}{(q-1)\sigma^2}+\frac{6kqU^2M_1^2\eta^2}{(q-1)\sigma^2}+\frac{2kqUM_1^2\eta^2}{(q-1)\sigma^2}+\frac{12k\wp UM_1^2\eta^2}{(q-1)\sigma^2}+\frac{4kqU^2M_2^2\eta^2}{(q-1)\sigma^4}$$
$$+\frac{3k\wp^2M_0M_1\eta^2}{\sigma}+\frac{6kU^2M_0M_1\eta^2}{\sigma}+\frac{6kUM_0M_1\eta^2}{\sigma}+\frac{24k\wp M_0M_2\eta^2}{\sigma^2}+\frac{14kU^2M_1M_2\eta^2}{\sigma^3}$$
$$+\frac{32kU^2M_1M_2\eta^2}{(q-1)\sigma^3}+\frac{8kq\wp M_1M_2\eta^2}{(q-1)\sigma^3}-\frac{3k\wp M_0M_1\eta^2}{\sigma}-\frac{9k\wp UM_1M_2\eta^2}{\sigma}-\frac{k\wp^2M_1^2\eta^2}{\sigma^2}$$
$$-\frac{6kU^2M_1^2\eta^2}{\sigma^2}-\frac{2kUM_1^2\eta^2}{\sigma^2}-\frac{4k\wp^2M_0M_2\eta^2}{\sigma^2}-\frac{24kU^2M_0M_2\eta^2}{\sigma^2}-\frac{8kUM_0M_2\eta^2}{\sigma^2}$$
$$-\frac{2k\wp^2M_1^2\eta^2}{(q-1)\sigma^2}-\frac{12kU^2M_1^2\eta^2}{(q-1)\sigma^2}-\frac{-4kUM_1^2\eta^2}{(q-1)\sigma^2}-\frac{6kq\wp M_1^2\eta^2}{(q-1)\sigma^2}-\frac{7k\wp UM_1M_2\eta^2}{\sigma^3}$$
$$-\frac{16kqU^2M_1M_2\eta^2}{(q-1)\sigma^3}-\frac{16k\wp UM_1M_2\eta^2}{(q-1)\sigma^3}-\frac{2kU^2M_2^2\eta^2}{\sigma^4}-\frac{8kU^2M_2^2\eta^2}{(q-1)\sigma^4}+aM_1^2-aqM_1^2$$
$$+\frac{\wp\Omega M_1^2}{\sigma}-3bM_0M_1^2+3bqM_0M_1^2-\wp\Omega M_0M_1+U\Omega M_0M_1-3bM_0^2M_2$$
$$-3bqM_0^2M_2+2aM_0M_2-2aqM_0M_2+\frac{2\wp\Omega M_0M_2}{\sigma}+\frac{3U\Omega M_1M_2}{\sigma^2}-\frac{2U\Omega M_1^2}{\sigma}-\frac{4U\Omega M_0M_2}{\sigma}=0,$$
$$-bM_1^3+bqM_1^3-\wp M_1^2+U\Omega M_1^2+\Omega M_1^2+\frac{3k\eta^2\wp^2M_1^2}{\sigma}+\frac{6k\eta^2U^2M_1^2}{\sigma}-\frac{3k\eta^2\wp M_1^2}{\sigma}$$
$$+\frac{6k\eta^2UM_1^2}{\sigma}-\frac{9k\eta^2\wp UM_1^2}{\sigma}+\frac{4k\eta^2\wp^2M_1^2}{(q-1)\sigma}-\frac{2kq\eta^2\wp^2M_1^2}{(q-1)\sigma}+\frac{8k\eta^2U^2M_1^2}{(q-1)\sigma}$$
$$-\frac{4kq\eta^2U^2M_1^2}{(q-1)\sigma}-\frac{4k\eta^2\wp M_1^2}{(q-1)\sigma}+\frac{2kq\eta^2\wp M_1^2}{(q-1)\sigma}+\frac{8k\eta^2UM_1^2}{(q-1)\sigma}-\frac{4kq\eta^2UM_1^2}{(q-1)\sigma}$$
$$-\frac{12k\eta^2\wp UM_1^2}{(q-1)\sigma}+\frac{6kq\eta^2\wp UM_1^2}{(q-1)\sigma}-2k\eta^2M_0M_1-2k\eta^2\wp^2M_0M_1-2k\eta^2U^2M_0M_1$$
$$+4k\eta^2\wp M_0M_1-4k\eta^2UM_0M_1+4k\eta^2\wp UM_0M_1+2aM_2M_1-2aqM_2M_1$$
$$+\frac{3\wp\Omega M_2M_1}{\sigma}-6bM_0M_2M_1+6bqM_0M_2M_1++\frac{30k\eta^2\wp UM_2M_1}{\sigma^2}+\frac{4kq\eta^2\wp^2M_2M_1}{(q-1)\sigma^2}$$
$$+\frac{24kq\eta^2U^2M_2M_1}{(q-1)\sigma^2}+\frac{8kq\eta^2UM_2M_1}{(q-1)\sigma^2}+\frac{48k\eta^2\wp UM_2M_1}{(q-1)\sigma^2}-\frac{6U\Omega M_2M_1}{\sigma}-\frac{5k\eta^2\wp^2M_2M_1}{\sigma^2}$$

$$-\frac{30k\eta^2U^2M_2M_1}{\sigma^2}-\frac{10k\eta^2UM_2M_1}{\sigma^2}-\frac{8k\eta^2\wp^2M_2M_1}{(q-1)\sigma^2}-\frac{48k\eta^2U^2M_2M_1}{(q-1)\sigma^2}-\frac{16k\eta^2UM_2M_1}{(q-1)\sigma^2}$$
$$-\frac{24kq\eta^2\wp UM_2M_1}{(q-1)\sigma^2}+\frac{2U\Omega M_2^2}{\sigma^2}+\frac{12k\eta^2U^2M_2^2}{\sigma^3}+\frac{32k\eta^2U^2M_2^2}{(q-1)\sigma^3}+\frac{8kq\eta^2\wp UM_2^2}{(q-1)\sigma^3}$$
$$-2\wp\Omega M_0M_2+2\Omega M_0M_2+2\Omega M_0M_2+\frac{10k\eta^2\wp^2M_0M_2}{\sigma}$$
$$+\frac{20k\eta^2U^2M_0M_2}{\sigma}+\frac{20k\eta^2UM_0M_2}{\sigma}-\frac{10k\eta^2\eta M_0M_2}{\sigma}-\frac{30k\eta^2\wp U^2M_0M_2}{\sigma}-\frac{6k\eta^2\wp UM_2^2}{\sigma^3}$$
$$-\frac{16k\eta^2\wp UM_2^2}{(q-1)\sigma^3}=0,$$

$$-2k\wp^2M_1^2\eta^2+\frac{kq\wp^2M_1^2\eta^2}{(q-1)}-2kU^2M_1^2\eta^2+\frac{kqU^2M_1^2\eta^2}{(q-1)}-2kM_1^2\eta^2$$
$$+\frac{kqM_1^2\eta^2}{q-1}+4k\wp M_1^2\eta^2++\frac{4k\wp M_1^2\eta^2}{q-1}-4kUM_1^2\eta^2+\frac{2kqUM_1^2\eta^2}{q-1}+4k\wp UM_1^2\eta^2+\frac{4k\wp UM_1^2\eta^2}{q-1}$$
$$-\frac{16kq\eta^2U^2M_2^2}{(q-1)\sigma^3}+\frac{24k\wp UM_2^2\eta^2}{\sigma^2}+\frac{4kq\wp^2M_2^2\eta^2}{(q-1)\sigma^2}+\frac{24kqU^2M_2^2\eta^2}{(q-1)\sigma^2}+\frac{8kqUM_2^2\eta^2}{(q-1)\sigma^2}+\frac{48k\wp UM_2^2v^2}{(q-1)\sigma^2}$$
$$-6k\wp^2M_0M_2\eta^2-6kU^2M_0M_2\eta^2-6kM_0M_2\eta^2+12k\wp M_0M_2\eta^2-12kUM_0M_2\eta^2$$
$$+12k\wp UM_0M_2\eta^2+\frac{13k\eta^2M_1M_2\eta^2}{\sigma}+\frac{26kU^2M_1M_2\eta^2}{\sigma}+\frac{26kUM_1M_2\eta^2}{\sigma}$$
$$+\frac{16k\wp^2M_1M_2\eta^2}{(q-1)\sigma}+\frac{32kU^2M_1M_2\eta^2}{(q-1)\sigma}+\frac{8kq\wp M_1M_2\eta^2}{(q-1)\sigma}+\frac{32kUM_1M_2\eta^2}{(q-1)\sigma}+\frac{24kq\wp UM_1M_2\eta^2}{(q-1)\sigma}$$
$$-\frac{2k\wp^2M_1^2\eta^2}{(q-1)}-\frac{2kU^2M_1^2\eta^2}{(q-1)}--\frac{2kM_1^2\eta^2}{(q-1)}-\frac{2kq\wp M_1^2\eta^2}{(q-1)}-\frac{4kUM_1^2\eta^2}{(q-1)}-\frac{2kq\wp M_1^2\eta^2}{(q-1)}$$
$$-\frac{13k\wp M_1M_2\eta^2}{\sigma}-\frac{39k\wp UM_1M_2\eta^2}{\sigma}-\frac{8kq\wp^2M_1M_2\eta^2}{(q-1)\sigma}-\frac{16kqU^2M_1M_2\eta^2}{(q-1)\sigma}$$
$$-\frac{16k\wp M_1M_2\eta^2}{(q-1)\sigma}-\frac{16kqUM_1M_2\eta^2}{(q-1)\sigma}-\frac{48k\wp UM_1M_2\eta^2}{(q-1)\sigma}-\frac{4k\wp^2M_2^2\eta^2}{\sigma^2}$$
$$-\frac{24kU^2M_2^2\eta^2}{\sigma^2}-\frac{8kUM_2^2\eta^2}{\sigma^2}-\frac{8k\wp^2M_2^2\eta^2}{(q-1)\sigma^2}-\frac{48kU^2M_2^2\eta^2}{(q-1)\sigma^2}$$
$$-\frac{16kUM_2^2\eta^2}{(q-1)\sigma^2}-\frac{24kq\wp UM_2^2\eta^2}{(q-1)\sigma^2}+aM_2^2-aqM_2^2+\frac{2\wp\Omega M_2^2}{\sigma}-3bM_0M_2^2+3bqM_0M_2^2$$
$$-3bM_1^2M_2+3bqM_1^2M_2-3\wp\Omega M_1M_2+3U\Omega M_1M_2+3\Omega M_1M_2-\frac{4U\Omega M_2^2}{\sigma}=0,$$

$$3bM_1M_2^2q-3bM_1M_2^2+\frac{10\eta^2k\wp^2M_2^2}{\sigma}-8\eta^2k\wp^2M_1M_2-\frac{30\eta^2k\wp UM_2^2}{\sigma}$$
$$+16\eta^2k\wp M_1M_2-\frac{10\eta^2k\wp M_2^2}{\sigma}+16\eta^2k\wp M_1M_2+\frac{20\eta^2kU^2M_2^2}{\sigma}-8\eta^2kU^2M_1M_2$$

$$
\begin{aligned}
&+\frac{20\eta^2 kUM_2^2}{\sigma}-16\eta^2 kUM_1M_2-8\eta^2 kM_1M_2+\frac{16\eta^2 k\wp^2 M_2^2}{(q-1)\sigma}-\frac{8\eta^2 k\wp^2 M_2^2 q}{(q-1)\sigma}\\
&+\frac{4\eta^2 k\wp^2 M_1M_2 q}{(q-1)}-\frac{8\eta^2 k\wp^2 M_1M_2}{(q-1)}+\frac{24\eta^2 k\wp UM_2^2 q}{(q-1)\sigma}-\frac{48\eta^2 k\wp UM_2^2}{(q-1)\sigma}\\
&+\frac{16\eta^2 k\wp UM_1M_2}{q-1}-\frac{8\eta^2 k\wp UM_1M_2 q}{q-1}+\frac{8\eta^2 k\wp M_2^2 q}{(q-1)\sigma}-\frac{16\eta^2 k\wp M_2^2}{(q-1)\sigma}+\frac{16\eta^2 k\wp M_1M_2}{q-1}\\
&-\frac{8\eta^2 k\wp M_1M_2 q}{q-1}+\frac{32\eta^2 kU^2 M_2^2}{(q-1)\sigma}-\frac{16\eta^2 kU^2 M_2^2 q}{(q-1)\sigma}+\frac{4\eta^2 kU^2 M_1M_2 q}{q-1}-\frac{8\eta^2 kU^2 M_1M_2}{q-1}\\
&+\frac{32\eta^2 kUM_2^2}{(q-1)\sigma}-\frac{16\eta^2 kUM_2^2 q}{(q-1)\sigma}+\frac{8\eta^2 kUM_1M_2 q}{q-1}-\frac{16\eta^2 kUM_1M_2}{q-1}\\
&+\frac{4\eta^2 kM_1M_2 q}{q-1}-\frac{8\eta^2 kM_1M_2}{q-1}-2\wp M_2^2+2UM_2^2\Omega+2M_2^2\Omega=0,
\end{aligned}
$$

$$
\begin{aligned}
&bM_2^3 q-bM_2^3-6\eta^2 k\wp M_2^2+12\eta^2 k\wp UM_2^2+12\eta^2 k\wp M_2^2-6\eta^2 kU^2 M_2^2-12\eta^2 kUM_2^2\\
&-6\eta^2 kM_2^2+\frac{4\eta^2 k\wp^2 M_2^2 q}{q-1}-\frac{8\eta^2 k\wp^2 M_2^2}{q-1}+\frac{16\eta^2 k\wp UM_2^2}{q-1}-\frac{8\eta^2 k\wp UM_2^2 q}{q-1}\\
&+\frac{16\eta^2 k\wp M_2^2}{q-1}-\frac{8\eta^2 k\wp M_2^2 q}{q-1}+\frac{4\eta^2 kU^2 M_2^2 q}{q-1}-\frac{8\eta^2 kU^2 M_2^2}{q-1}\\
&+\frac{8\eta^2 kUM_2^2 q}{q-1}-\frac{16\eta^2 kUM_2^2}{q-1}+\frac{4\eta^2 kM_2^2 q}{q-1}-\frac{8\eta^2 kM_2^2}{q-1}=0.
\end{aligned}
$$

By solving the above system in $M_0, M_1, M_{2,} a, k$ we have two sets of solutions.

Set 1.

$$
\begin{aligned}
M_0=&\frac{(\wp^2-2\wp U+2(U-1)U)\sqrt{b^2(q-1)^2(q+1)^2(q+3)^2\Omega^2(\wp^2-4U)(\wp-2U)^2(-\wp+U+1)^2}}{b^2(q-1)^2(q+3)^2\sigma(\wp^2-4U)(\wp-U-1)(\wp-2U)}\\
&-\frac{b(q-1)(q+1)(q+3)\Omega(\wp-2U)^2}{b^2(q-1)^2(q+3)^2\sigma(\wp-2U)},
\end{aligned}
$$

$$
M_1=\frac{2(\frac{\sqrt{b^2(q-1)^2(q+1)^2(q+3)^2\Omega^2(\wp^2-4U)(\wp-2U)^2(-\wp+U+1)^2}}{\wp^2-4U}+b(q-1)(q+1)(q+3)\Omega(\wp-U-1)}{b^2(q-1)^2(q+3)^2},
$$

$$M_2=-\frac{2(q+1)^2\sigma\Omega^2(\wp-2U)(\wp-U-1)^3}{\sqrt{b^2(q-1)^2(q+1)^2(q+3)^2\Omega^2(\wp^2-4U)(\wp-2U)^2(-\wp+U+1)^2}},$$

$$k=-\frac{b(q-1)^2(q+1)\sigma\Omega^2(\wp-2U)(\wp-U-1)}{\eta^2\sqrt{b^2(q-1)^2(q+1)^2(q+3)^2\Omega^2(\wp^2-4U)(\wp-2U)^2(-\wp+U+1)^2}},$$

$$a=-\frac{2\sqrt{b^2(q-1)^2(q+1)^2(q+3)^2\Omega^2(\wp^2-4U)(\wp-2U)^2(-\wp+U+1)^2}}{b(q-1)^2(q+3)\sigma(\wp-2U)(\wp-U-1)}$$

Set 2.

$$M_0=\frac{(\wp^2-2\wp U+2(U-1)U)\sqrt{b^2(q-1)^2(q+1)^2(q+3)^2\Omega^2(\wp^2-4U)(\wp-2U)^2(-\wp+U+1)^2}}{b^2(q-1)^2(q+3)^2\sigma(\wp-2U)(\wp^2-4U)(\wp-U-1)}-\frac{b(q-1)(q+1)(q+3)\Omega(\wp-2U)^2}{b^2(q-1)^2(q+3)^2\sigma(\wp-2U)},$$

$$M_1=\frac{2\left(b(q-1)(q+1)(q+3)\Omega(\wp-U-1)-\frac{\sqrt{b^2(q-1)^2(q+1)^2(q+3)^2\Omega^2(\wp^2-4U)(\wp-2U)^2(-\wp+U+1)^2}}{\wp^2-4U}\right.}{b^2(q-1)^2(q+3)^2}$$

$$M_2=\frac{2(q+1)^2\sigma\Omega^2(\wp-2U)(\wp-U-1)^3}{\sqrt{b^2(q-1)^2(q+1)^2(q+3)^2\Omega^2(\wp^2-4U)(\wp-2U)^2(-\wp+U+1)^2}},$$

$$k=\frac{b(q-1)^2(q+1)\sigma\Omega^2(\wp-2U)(\wp-U-1)}{\eta^2\sqrt{b^2(q-1)^2(q+1)^2(q+3)^2\Omega^2(\wp^2-4U)(\wp-2U)^2(-\wp+U+1)^2}},$$

$$a=\frac{2\sqrt{b^2(q-1)^2(q+1)^2(q+3)^2\Omega^2(\wp^2-4U)(\wp-2U)^2(-\wp+U+1)^2}}{b(q-1)^2(q+3)^2\sigma(\wp-2U)(\wp-U-1)}$$

By substituting from above two sets into (19) with (17), we get the solution $U(\xi)$ of (7), and by putting it into (5) with equation (6), we obtain the solution of (2) as:

Class 1. When $H=\wp^2-4U>0,$

$$\begin{aligned}u(x,t)=(M_0&\\+M_1(&\frac{\left[\wp(p_2-p_1)-\sqrt{H}(p_2+p_1)\right]\sinh(\frac{\sqrt{H}\xi}{2\sigma})+\left[\wp(p_2+p_1)-\sqrt{H}(p_2-p_1)\right]\cosh(\frac{\sqrt{H}\xi}{2\sigma})}{\sigma\left[(\wp-2)(p_2-p_1)-\sqrt{H}(p_2+p_1)\right]\sinh(\frac{\sqrt{H}\xi}{2\sigma})+\sigma\left[(\wp-2)(p_2+p_1)-\sqrt{H}(p_2-p_1)\right]\cosh(\frac{\sqrt{H}\xi}{2\sigma})})\\+M_2(&\frac{\left[\wp(p_2+p_1)-\sqrt{H}(p_2+p_1)\right]\sinh(\frac{\sqrt{H}\xi}{2\sigma})+\left[\wp(p_2+p_1)-\sqrt{H}(p_2-p_1)\right]\cosh(\frac{\sqrt{H}\xi}{2\sigma})}{\sigma\left[(\wp-2)(p_2-p_1)-\sqrt{H}(p_2+p_1)\right]\sinh(\frac{\sqrt{H}\xi}{2\sigma})+\sigma\left[(\wp-2)(p_2-p_1)-\sqrt{H}(p_2-p_1)\right]\cosh(\frac{\sqrt{H}\xi}{2\sigma})})\end{aligned}\qquad(20)$$

within the confines: $r^2 + p_1^2 + p_2^2 \neq 0.$

$$u(x,t) = (M_0 + M_1(\frac{\wp - 2U}{2\sigma(\wp - U - 1)} - \frac{\sqrt{H}}{2\sigma(\wp - U - 1)}\tanh(\frac{\sqrt{H}(\xi)}{2\sigma})) + M_2(\frac{\wp - 2U}{2\sigma(\wp - U - 1)} - \frac{\sqrt{H}}{2\sigma(\wp - U - 1)}\tanh(\frac{\sqrt{H}(\xi)}{2\sigma}))^2)^{\frac{1}{q-1}}, \tag{21}$$

within the confines: $(\wp - 2)(p_2 - p_1) - \sqrt{H}(p_2 + p_1) = 0.$

$$u(x,t) = (M_0 + M_1(\frac{\wp - 2U}{2\sigma(\wp - U - 1)} - \frac{\sqrt{H}}{2\sigma(\wp - U - 1)}\coth(\frac{\sqrt{H}\xi}{2\sigma})) + M_2(\frac{\wp - 2U}{2\sigma(\wp - U - 1)} - \frac{\sqrt{H}}{2\sigma(\wp - U - 1)}\coth(\frac{\sqrt{H}\xi}{2\sigma}))^2)^{\frac{1}{q-1}}, \tag{22}$$

within the confines: $(\wp - 2)(p_2 + p_1) - \sqrt{H}(p_2 - p_1) = 0,$ where

$$\xi = \eta x - \Omega t. \tag{23}$$

Class 2. When $H = \wp^2 - 4U < 0,$

$$u(x,t) = (M_0 + M_1(\frac{(\wp p_1 - \sqrt{-H}p_2)\cos(\frac{\sqrt{-H}\xi}{2\sigma}) + (\wp p_2 + \sqrt{-H}p_1)\sin(\frac{\sqrt{-H}\xi}{2\sigma})}{\sigma((\wp - 2)p_1 - \sqrt{-H}p_2)\cos(\frac{\sqrt{-H}\xi}{2\sigma}) + \sigma((\wp - 2)p_2 + \sqrt{-H}p_1)\sin(\frac{\sqrt{-H}\xi}{2\sigma})}) + M_2(\frac{(\wp p_1 - \sqrt{-H}p_2\cos(\frac{\sqrt{-H}\xi}{2\sigma}) + (\wp p_2 + \sqrt{-H}p_1)\sin(\frac{\sqrt{-H}\xi}{2\sigma})}{\sigma((\wp - 2)p_1 - \sqrt{-H}p_2)\cos(\frac{\sqrt{-H}\xi}{2\sigma}) + \sigma((\wp - 2)p_2 + \sqrt{-H}p_1)\sin(\frac{\sqrt{-H}\xi}{2\sigma})})^2)^{\frac{1}{q-1}}, \tag{24}$$

within the confines: $r^2 + p_1^1 + p_2^2 \neq 0.$

$$u(x,t) = (M_0 + M_1(\frac{\wp - 2U}{2\sigma(\wp - U - 1)} + \frac{\sqrt{-H}}{2\sigma(\wp - U - 1)}\tan(\frac{\sqrt{-H}(x - c_1 t)}{2\sigma})) + M_2(\frac{\wp - 2U}{2\sigma(\wp - U - 1)} + \frac{\sqrt{-H}}{2\sigma(\wp - U - 1)}\tanh(\frac{\sqrt{-H}(x - c_1 t)}{2\sigma}))^2)^{\frac{1}{q-1}}, \tag{25}$$

within the confines: $(\wp - 2)p_2 + \sqrt{-H}p_1 = 0,$

$$u(x,t)=\left(M_0+M_1\left(\frac{\wp-2U}{2\sigma(\wp-U-1)}+\frac{\sqrt{-H}}{2\sigma(\wp-U-1)}\cot\left(\frac{\sqrt{-H}\,(x-c_1t)}{2\sigma}\right)\right)\right)$$
$$+M_2\left(\left(\frac{\wp-2U}{2\sigma(\wp-U-1)}+\frac{\sqrt{-H}}{2\sigma(\wp-U-1)}\cot\left(\frac{\sqrt{-H}\,(x-c_1t)}{2\sigma}\right)\right)^2\right)^{\frac{1}{q-1}}, \tag{26}$$

within the confines: $(\wp-2)p_1-\sqrt{-H}\,p_2=0,$ where

$$\xi=\eta x-\Omega t. \tag{27}$$

4. GRAPHICAL ILLUSTRATIONS

We present a series of graphical illustrations that visually demonstrate the relationships between various equations and their corresponding solutions. Fig. 1 showcases the graph of Eq. (21) in conjunction with Eq. (23), both obtained using the $\left(\frac{\varsigma'}{k\varsigma'+G+r}\right)$ expansion method. The specific parameter values used for this graph include. $b=0.2, v=0.1,\ \tau=0.3,\ U=0.001,\ q=3,\ \sigma=0.2,\ \Omega=0.1.$

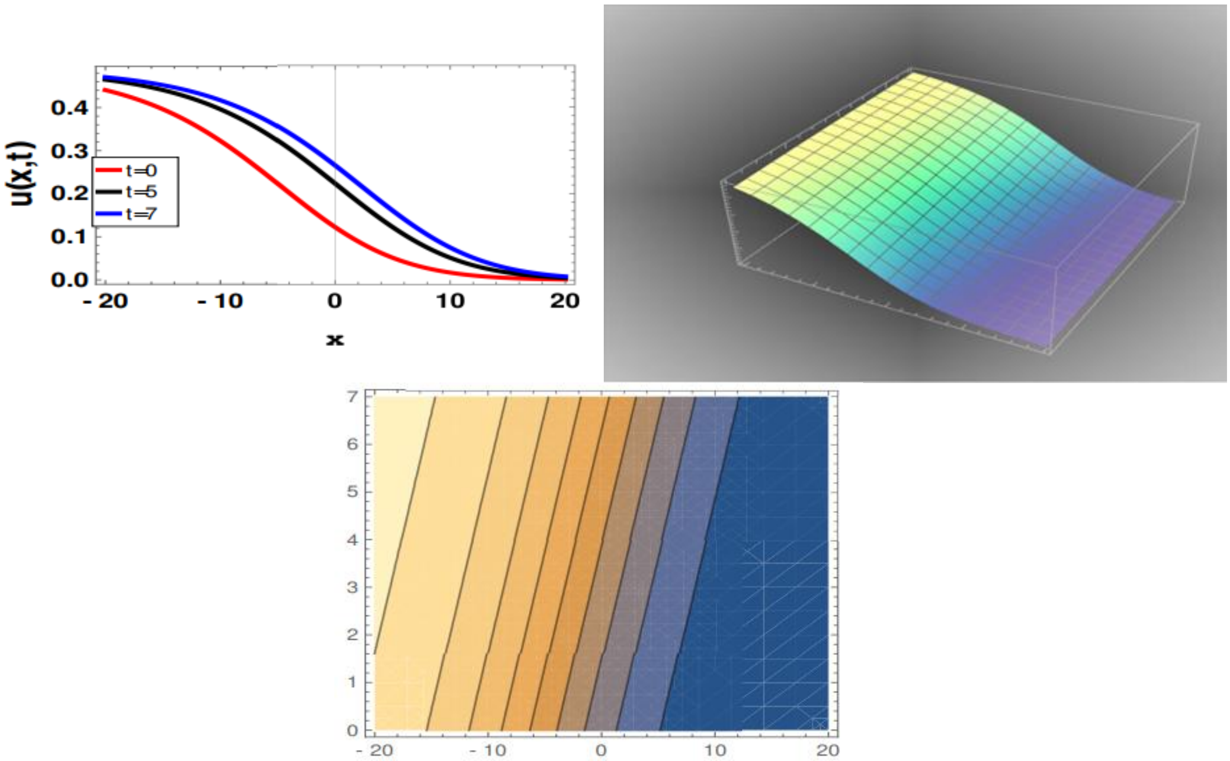

Figure 1. Graph of (21) with (23) at *b* = 0.2, *η* = 0.1, *L* = 0.3, *U* = 0.001, *q* = 3, *σ* = 0.2, Ω = 0.1.

Moving on to Fig. 2, we present the graph of Eq. (25) along with Eq. (27), which were also derived using the $\left(\dfrac{\varsigma'}{k\varsigma'+G+r}\right)$ expansion method. The parameter values for this case are $b=0.01,\ \nu=0.1,\ \tau=0.001,\ U=0.001,\ q=3,\ \sigma=0.3,\ \Omega=0.1.$

These graphical representations provide a visual depiction of the solutions obtained from the respective equations and methods employed. They offer further insights into the behavior and characteristics of the systems under consideration, allowing for a better understanding of their dynamics and properties.

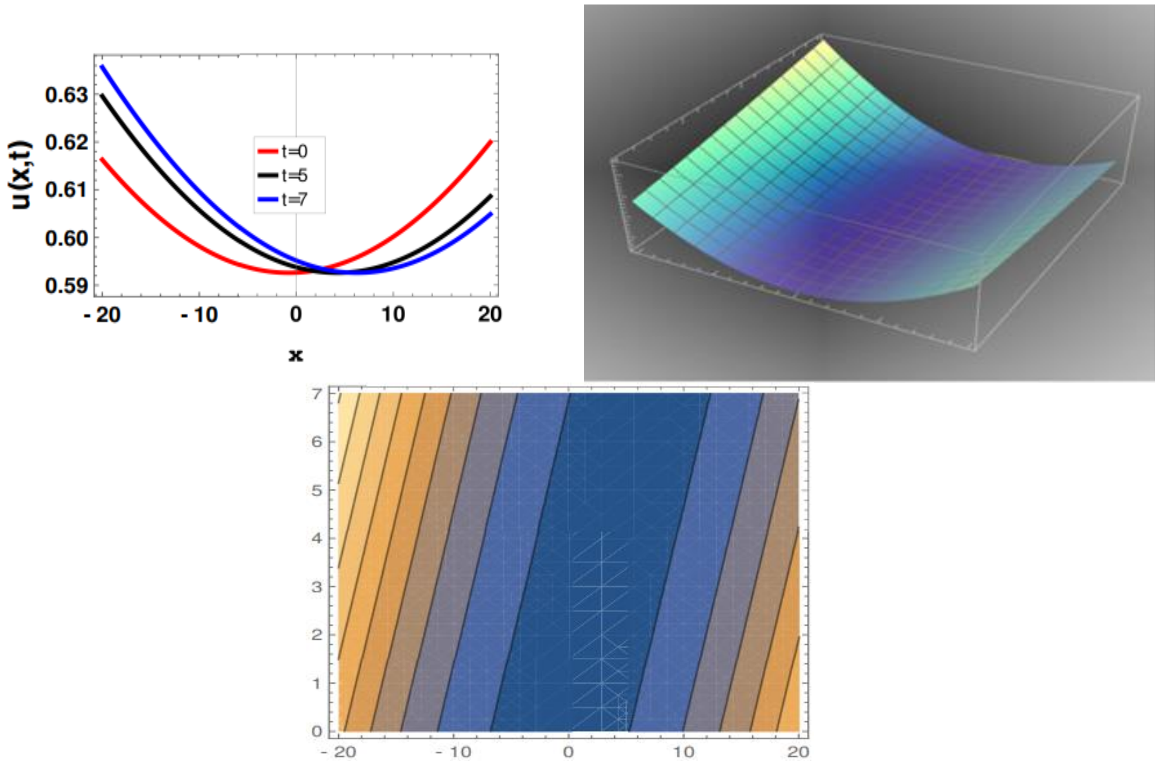

Figure 2. Graph of (25) with (27) at *b* = 0.01, *η* = 0.1, *L* = 0.001, *U* = 0.001, *q* = 3, *σ* = 0.3, Ω = 0.1.

5. APPLICATION OF NUMERICAL METHOD TO EQUATION

In this section, we address the mathematical problem denoted by Eq. (2) in the presence of given septic B-splines. Among many numerical methods, the collocation method is a method that gives good results and is very convenient in terms of time and workload. In this method $u_{numeric}(x,t)$ conforms with the $u_{exact}(x,t)$ is written as follows:

$$u_{numeric}(x,t)=\sum_{m=-3}^{N+3}\phi_m(x)\sigma_m(t). \tag{28}$$

When $h\zeta=x-x_m,\quad 0\le\zeta\le1,$ transformation is used, the region $[x_m,x_{m+1}]$ turns to an interval of [0, 1]. Accordingly, B-splines that rely on ζ over the finite element $[0,1]$ are explained as follows:

$$
\begin{aligned}
&\phi_{m-3} = 1-7\zeta+21\zeta^2-35\zeta^3+35\zeta^4-21\zeta^5+7\zeta^6-\zeta^7,\\
&\phi_{m-2} = 120-392\zeta+504\zeta^2-280\zeta^3+84\zeta^5-42\zeta^6+7\zeta^7,\\
&\phi_{m-1} = 1191-1715\zeta+315\zeta^2+665\zeta^3-315\zeta^4-105\zeta^5+105\zeta^6-21\zeta^7,\\
&\phi_{m} = 2416-1680\zeta+560\zeta^4-140\zeta^6+35\zeta^7,\\
&\phi_{m+1} = 1191+1715\zeta+315\zeta^2-665\zeta^3-315\zeta^4+105\zeta^5+105\zeta^6-35\zeta^7,\\
&\phi_{m+2} = 120+392\zeta+540\zeta^2+280\zeta^3-84\zeta^5-42\zeta^6-21\zeta^7,\\
&\phi_{m+3} = 1+7\zeta+21\zeta^2+35\zeta^3+35\zeta^4+21\zeta^5+7\zeta^6-7\zeta^7,\\
&\phi_{m+4} = \zeta^7.
\end{aligned} \tag{29}
$$

The following is the form of u_m 's nodal values and their derivatives:

$$
\begin{aligned}
u_m^{'} &= \frac{7}{h}\left(-\sigma_{m-3}-56\sigma_{m-2}-245\sigma_{m-1}+245\sigma_{m+1}+56\sigma_{m+2}+\sigma_{m+3}\right),\\
u_m^{''} &= \frac{42}{h^2}\left(\sigma_{m-3}+24\sigma_{m-2}+15\sigma_{m-1}-80\sigma_m+15\sigma_{m+1}+24\sigma_{m+2}+\sigma_{m+3}\right),\\
u_m^{'''} &= \frac{210}{h^3}\left(-\sigma_{m-3}-8\sigma_{m-2}+19\sigma_{m-1}-19\sigma_{m+1}+8\sigma_{m+2}+\sigma_{m+3}\right).
\end{aligned} \tag{30}
$$

Now, placing (28) and (29) in Eq.(2), the following general system of ODEs are obtained:

$$
\begin{aligned}
u_m^{'} &= \frac{7}{h}\left(-\sigma_{m-3}-56\sigma_{m-2}-245\sigma_{m-1}+245\sigma_{m+1}+56\sigma_{m+2}+\sigma_{m+3}\right),\\
u_m^{''} &= \frac{42}{h^2}\left(\sigma_{m-3}+24\sigma_{m-2}+15\sigma_{m-1}-80\sigma_m+15\sigma_{m+1}+24\sigma_{m+2}+\sigma_{m+3}\right),\\
u_m^{'''} &= \frac{210}{h^3}\left(-\sigma_{m-3}-8\sigma_{m-2}+19\sigma_{m-1}-19\sigma_{m+1}+8\sigma_{m+2}+\sigma_{m+3}\right).
\end{aligned} \tag{30}
$$

$$
\begin{aligned}
&\dot{\sigma}_{m-3}+120\dot{\sigma}_{m-2}+1191\dot{\sigma}_{m-1}+2416\dot{\sigma}_{m}+1191\dot{\sigma}_{m+1}+120\dot{\sigma}_{m+2}+\dot{\sigma}_{m+2}\\
&=\frac{42}{h^2}\left(\sigma_{m-3}+24\sigma_{m-2}+15\sigma_{m-1}-80\sigma_m+15\sigma_{m+1}+24\sigma_{m+2}+\sigma_{m+3}\right)\\
&+2\left(2-3Z_m\right)\left(\sigma_{m-3}+120\sigma_{m-2}+1191\sigma_{m-1}+2416\sigma_m+1191\sigma_{m+1}+120\sigma_{m+2}+\sigma_{m+3}\right),
\end{aligned} \tag{31}
$$

where $\dot{\sigma}=\dfrac{d\sigma}{dt}$ and

$$Z_m = u = \sigma_{m-3}+120\sigma_{m-2}+1191\sigma_{m-1}+2416\sigma_m+1191\sigma_{m+1}+120\sigma_{m+2}+\sigma_{m+3}.$$

In Eq. (31), substituting $\dot{\sigma}_i$ by forward difference approximation $\dot{\sigma}_i=\dfrac{\sigma_i^{n+1}-\sigma_i^n}{\Delta t}$ and σ_i by Crank–Nicolson formulation $\dot{\sigma}_i=\dfrac{\sigma_i^{n+1}+\sigma_i^n}{\Delta t}$ then

$$
\begin{aligned}
&\lambda_1\sigma_{m-3}^{n+1}+\lambda_2\sigma_{m-2}^{n+1}+\lambda_3\sigma_{m-1}^{n+1}+\lambda_4\sigma_{m}^{n+1}+\lambda_5\sigma_{m+1}^{n+1}+\lambda_6\sigma_{m+2}^{n+1}+\lambda_7\sigma_{m+3}^{n+1}\\
&=\lambda_7\sigma_{m-3}^{n}+\lambda_6\sigma_{m-2}^{n}+\lambda_5\sigma_{m-1}^{n}+\lambda_4\sigma_{m}^{n}+\lambda_3\sigma_{m+1}^{n}+\lambda_2\sigma_{m+2}^{n}+\lambda_1\sigma_{m+3}^{n+1},
\end{aligned}
\tag{32}
$$

where

$$
\begin{aligned}
&\lambda_1=\left[1-A-B\right],\\
&\lambda_2=\left[120-24A120B\right],\\
&\lambda_3=\left[1191-15A-1191B\right],\\
&\lambda_4=\left[2416+80A-2416B\right],\\
&\lambda_5=\left[1191+15A+1191B\right],\\
&\lambda_6=\left[120+24A+120B\right],\\
&\lambda_7=\left[1+A+B\right],\\
&A=\frac{21}{h^2}\Delta t,\quad B=\frac{(2-3Z_m)}{2}\Delta t
\end{aligned}
\tag{33}
$$

system of linear equations are generated. Unknown parameters $\sigma_{-3},\sigma_{-2},\sigma_{-1},\sigma_{N+1},\sigma_{N+2}$ and σ_{N+3} must be eliminated from the system (32) in order to guarantee a unique solution.

6. STABILITY ANALYSIS

Stability analysis was done using the Von-Neumann theory. A typical Fourier mode of amplitude's amplification factor, ξ, can be found as follows [33]:

$$\sigma_m^n=\xi^n e^{imkh}. \tag{34}$$

Using (34) in the iterative system (32),

$$\xi=\frac{p_1+ip_2}{p_1-ip_2} \tag{35}$$

is obtained and in which

$$
\begin{aligned}
p_1&=2\cos(3kh)+240\cos(2kh)+2382\cos(kh)+2416+80A-2416B,\\
p_2&=(2A+2B)\sin(3kh)+(48A+240B)\sin(2kh)+(30A+2382B)\sin(kh).
\end{aligned}
\tag{36}
$$

It is observed that the maximum values of is $|\xi|=1$, affirming the stability of the linearized scheme (36).

7. NUMERICAL EXPERIMENTS AND DISCUSSIONS

Examples are provided in this part to show the productivity and resilience of the suggested numerical approach. For a nonlinear initial and boundary value problem having an exact solution, the L_2 and L_∞ error norms are defined as [34-37]:

$$L_2 = \left\| u^{exact} - u_N \right\|_2 \simeq \sqrt{h \sum_{j=1}^{N} \left| u_j^{exact} - (u_N)_j \right|^2} \tag{37}$$

$$L_\infty = \left\| u^{exact} - u_N \right\|_\infty \simeq \max_j \left| u_j^{exact} - (u_N)_j \right|, \quad j = 1, 2, ..., N. \tag{38}$$

7.1. TEST PROBLEM 1

The N-W-S equation is discussed for the parameters $k=1, a=2, b=3$ and $q=2$, so the equation has the following exact solution:

$$u(x,t) = \frac{-\frac{2}{3}\lambda e^{2t}}{-\frac{2}{3} + \lambda - \lambda e^{2t}}, \tag{39}$$

with the following initial and boundary conditions:

$$u(x,0) = \lambda \tag{40}$$

where $u \to 0 \ as \ x \to \pm\infty.$

To demonstrate the precision of the numerical scheme, the equation is investigated over the domain $[x_L = 0, \ x_R = 1]$ until time $t = 1$. In numerical experiments, $\Delta t = 10^{-4}$ with $h = 0.1$ and 0.02 have been selected in accordance with the references to be compared $\lambda = 0.03$. The corresponding findings are detailed in Table 1, and the solutions are listed in Table 2, have been compared with multiquadrics (MQ) and Gaussian (GA) methods [38]. It has been noted that, compared to the previous approaches, the current scheme in conjunction with the division schemes is superior and more reliable. Three-dimensional cases of solutions are created at selected time intervals from Fig. 3.

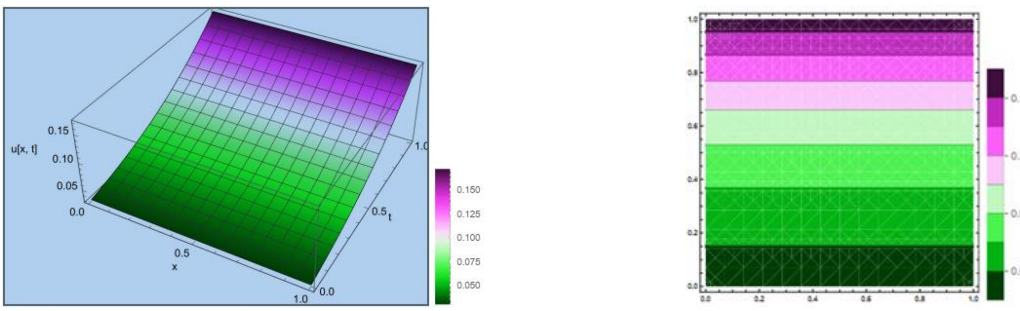

Figure 3. Numerical solutions and contour lines for test problem 1.

Table 1. Error norms for test problem 1.

$\lambda = 0.03$	$\Delta t = 0.0001$	$h = 0.1$	$\Delta t = 0.0001$	$h = 0.02$
t	L_2	L_∞	L_2	L_∞
0.001	2.840×10^{-7}	2.714×10^{-7}	5.427×10^{-7}	2.708×10^{-7}
0.002	5.697×10^{-7}	5.441×10^{-7}	10.87×10^{-7}	5.432×10^{-7}
0.003	8.570×10^{-7}	8.180×10^{-7}	16.36×10^{-7}	8.173×10^{-7}
0.004	11.46×10^{-7}	10.93×10^{-7}	21.88×10^{-7}	10.93×10^{-7}
0.005	14.36×10^{-7}	13.70×10^{-7}	27.45×10^{-7}	13.70×10^{-7}
0.006	17.28×10^{-7}	16.49×10^{-7}	33.04×10^{-7}	16.49×10^{-7}
0.007	20.23×10^{-7}	19.31×10^{-7}	38.66×10^{-7}	19.29×10^{-7}
0.008	23.19×10^{-7}	22.12×10^{-7}	44.31×10^{-7}	22.11×10^{-7}
0.009	26.16×10^{-7}	24.95×10^{-7}	50.00×10^{-7}	24.95×10^{-7}
0.01	29.15×10^{-7}	27.81×10^{-7}	55.72×10^{-7}	27.80×10^{-7}
0.05	16.38×10^{-6}	15.62×10^{-6}	31.30×10^{-6}	15.61×10^{-6}
0.1	37.91×10^{-5}	36.15×10^{-5}	36.50×10^{-5}	36.14×10^{-5}
0.5	36.38×10^{-5}	58.53×10^{-5}	59.11×10^{-5}	58.52×10^{-5}
1.0	51.91×10^{-5}	49.50×10^{-5}	49.99×10^{-5}	49.50×10^{-5}

7.2. TEST PROBLEM 2

When $k=1,\ a=3,\ b=4$ and $q=3$ are taken in Eq.(2), the exact solution form of the N-W-S equation is

$$u(x,t)=\sqrt{\frac{3}{4}}\frac{e^{\sqrt{6}x}}{e^{\sqrt{6}x}+e^{(\frac{\sqrt{6}}{2}x-\frac{9}{2}t)}}, \tag{41}$$

with the following initial and boundary conditions:

$$u(x,0)=\sqrt{\frac{3}{4}}\frac{e^{\sqrt{6}x}}{e^{\sqrt{6}x}+e^{(\frac{\sqrt{6}}{2}x)}}. \tag{42}$$

where $u \to 0\ as\ x \to \pm\infty.$

The time step is chosen as $t=10^{-3}$. Typical values in simulation computations $\Delta t=10^{-4}$ and 10^{-3} with $h=0.1$ and 0.01 are selected.

Table 2. A comparison of the error norms for test problem 1.

$\boldsymbol{\lambda = 0.03 \quad \Delta t = 0.05 \quad h = 0.1}$		
$\boldsymbol{t}$	$\boldsymbol{L_2}$	$\boldsymbol{L_\infty}$
FEM 0.1	3.8552×10^{-5}	3.6758×10^{-5}
$(MQ^{[38]})0.1$	3.1077×10^{-3}	1.2942×10^{-3}
$(GA^{[38]})0.1$	3.5530×10^{-3}	1.4342×10^{-3}
FEM 0.2	1.0320×10^{-4}	9.8400×10^{-5}
$(MQ^{[38]})0.2$	4.8523×10^{-3}	2.0761×10^{-3}
$(GA^{[38]})0.2$	5.2482×10^{-3}	2.2271×10^{-3}
FEM 0.3	2.0740×10^{-4}	1.9775×10^{-4}
$(MQ^{[38]})0.3$	5.9488×10^{-3}	2.5696×10^{-3}
$(GA^{[38]})0.3$	6.1387×10^{-3}	2.6549×10^{-3}
FEM 0.4	3.7067×10^{-4}	3.5342×10^{-4}
$(MQ^{[38]})0.4$	6.7126×10^{-3}	2.9144×10^{-3}

$\lambda = 0.03$ $\Delta t = 0.05$ $h = 0.1$		
t	L_2	L_∞
$(GA^{[38]})0.4$	6.6374×10^{-3}	2.9048×10^{-3}
FEM 0.5	6.2100×10^{-4}	5.9210×10^{-4}
$(MQ^{[38]})0.5$	7.2797×10^{-3}	3.1718×10^{-3}
$(GA^{[38]})0.5$	6.9229×10^{-3}	3.0583×10^{-3}

Table 3 presents the values of the L_2 and L_∞ error norms calculated over these values for time levels and step sizes. When the tables were examined, it was observed that the calculated L_2 and L_∞ error norms were marginally small.

Table 3. Error norms for test problem 2.

	$\Delta t = 0.0001$	$h = 0.1$	$\Delta t = 0.001$	$h = 0.1$
t	L_2	L_∞	L_2	L_∞
0.0002	27.25×10^{-6}	25.99×10^{-6}	27.33×10^{-5}	26.05×10^{-5}
0.0004	54.53×10^{-6}	51.99×10^{-6}	54.82×10^{-5}	52.27×10^{-5}
0.0006	81.82×10^{-6}	78.02×10^{-6}	82.48×10^{-5}	78.64×10^{-5}
0.0008	10.91×10^{-5}	10.41×10^{-5}	11.03×10^{-4}	10.51×10^{-4}
0.0010	13.64×10^{-5}	13.01×10^{-5}	13.83×10^{-4}	13.18×10^{-4}
	$\Delta t = 0.0001$	$h = 0.01$	$\Delta t = 0.0001$	$h = 0.01$
	L_2	L_∞	L_2	L_∞
0.0002	26.15×10^{-6}	25.99×10^{-6}	26.18×10^{-4}	26.04×10^{-4}
0.0004	52.25×10^{-6}	51.99×10^{-6}	52.53×10^{-4}	52.27×10^{-4}
0.0006	78.40×10^{-6}	78.01×10^{-6}	79.04×10^{-4}	78.64×10^{-4}
0.0008	10.45×10^{-5}	10.40×10^{-5}	10.57×10^{-3}	10.51×10^{-3}
0.0010	13.07×10^{-5}	13.01×10^{-5}	13.25×10^{-3}	13.18×10^{-3}

In Fig. 4, the three-dimensional wave solutions produced at the chosen time intervals can be clearly seen.

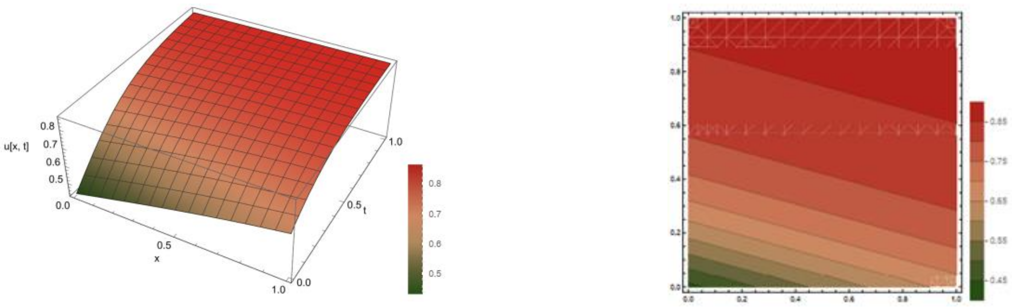

Figure 4. Numerical solutions and contour line for test problem 2.

7.3. TEST PROBLEM 3

When $k=1, a=1, b=1$ and $q=3$ are taken in Eq. (2), the equation turns into the Allen-Cahn equation, which has the following form

$$u_t = u_{xx} + u - u^3,$$

with the exact solution as

$$u(x,t) = -0.5 + 0.5\tanh(0.3536x - 0.75t)$$

and the initial condition

$$u(x,0) = -0.5 + 0.5\tanh(0.3536x).$$

The region of the problem is selected as $[x_L = 0, x_R = 1]$. In simulation calculations as common values $\Delta t = 10^{-4}$ with $h = 0.1$ and 0.01 are chosen. Table 4 contains a tabulation of the results collected. The table unequivocally demonstrates how tiny the error norms produced by our approach are. One could argue that the numerical results are positively impacted by the addition of more time divisions. As anticipated for $h = 0.1$ and $\Delta t = 0.0001$ Fig. (5), the numerical solutions to the problem overlap.

Table 4. Error norms for test problem 3.

	$\Delta t = 0.0001$	$h = 0.1$	$\Delta t = 0.0001$	$h = 0.01$
t	L_2	L_∞	L_2	L_∞
0.0001	54.01×10^{-6}	94.57×10^{-6}	84.94×10^{-7}	31.07×10^{-6}
0.0002	80.31×10^{-6}	14.91×10^{-5}	15.93×10^{-6}	43.39×10^{-6}
0.0003	94.47×10^{-6}	18.41×10^{-5}	23.61×10^{-6}	55.80×10^{-6}
0.0004	10.33×10^{-5}	20.92×10^{-5}	31.37×10^{-6}	68.29×10^{-6}
0.0005	11.01×10^{-5}	22.91×10^{-5}	39.19×10^{-6}	80.85×10^{-6}
0.0006	11.59×10^{-5}	24.61×10^{-5}	47.04×10^{-6}	93.47×10^{-6}
0.0007	12.16×10^{-5}	26.15×10^{-5}	54.93×10^{-6}	10.61×10^{-5}
0.0008	12.73×10^{-5}	27.58×10^{-5}	62.85×10^{-6}	11.88×10^{-5}
0.0009	13.31×10^{-5}	28.94×10^{-5}	70.80×10^{-6}	13.16×10^{-5}
0.0010	13.91×10^{-5}	30.26×10^{-5}	78.79×10^{-6}	13.89×10^{-5}

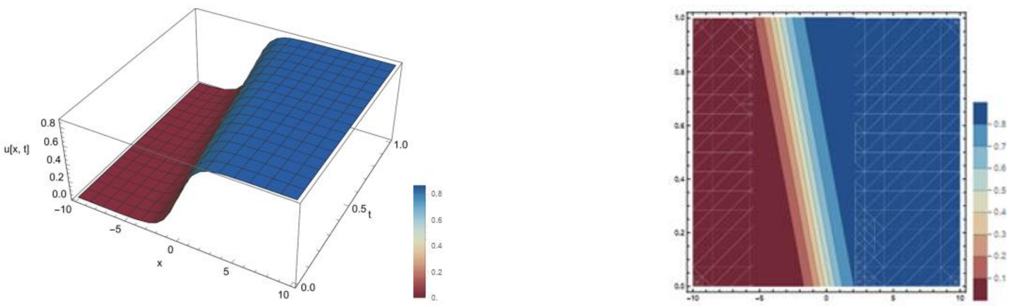

Figure 5. Numerical solutions and contour line for test problem 3.

8. CONCLUSION

In this work, the N-W-S equation is inclusively analyzed by using two robust and efficient methods. Firstly, the general form of the $\left(\dfrac{\varsigma'}{k\varsigma' + G + r}\right)$ expansion method has been used for the exact solutions, and secondly, the collocation method has been used for numerical solutions of the equation. The stability of the numerical algorithm has been thoroughly controlled using the von Neumann method, and it has been demonstrated to be unconditionally

stable. L_2 and L_∞ error norms have been assessed in order to evaluate the effectiveness and validity of numerical algorithms. For the sake of a better understanding of the obtained solutions, some graphical illustrations are also presented for the two methods. Exact and numerical experiments proved that the results are achieved from the current methods are productive, credible, fruitful, and vigorous. Besides, the performance of the numerical method is in good agreement with some earlier results from the literature. There are several uses for these new findings in physics and other applied scientific fields. To sum up, the techniques discussed here are useful, effective, and executable mathematical tools for resolving nonlinear PDEs.

REFERENCES

[1] Saravanan, A., Magesh, N., *Journal of the Egyptian Mathematical Society*, **21**(3), 259, 2013.
[2] Kelkar, A., Yomba, E., Djellouli, R., *Communications in Nonlinear Science and Numerical Simulation*, **41**, 118, 2016.
[3] Newell, A., Whitehead, J.A., *Journal of Fluid Mechanics***, 38**(2), 279, 1969.
[4] Segel, L.A., *Journal of Fluid Mechanics*, **38**(1), 203, 1969.
[5] Allen, S.M., Cahn, J. W., *Acta Metallurgica*, **27**(6), 1085, 1979.
[6] Voigt, A., *Applicable Analysis*, **81**(4), 1283, 2002.
[7] FitzHugh, R., *Bulletin of Mathematical Biology*, **17**(4), 257, 1995.
[8] Nagumo, J., Arimoto, S., Yoshizawa, S., *Proceedings of the IRE*, **50**(10), 2061, 1962.
[9] Aasaraai, A., *Middle East Journal of Scientific Research*, **10**(2), 270, 2011.
[10] Ezzati, R., Shakibi, K., *Procedia Computer Science*, **3**, 1043, 2011.
[11] Mourazar, S.S., Soori, M., Nazari-Golsham, A., *Australian Journal of Basic and Applied Sciences*, **5,** 1400, 2011.
[12] Macias-Diaz, E., Ruiz-Ramirez, J., *Applied Numerical Mathematics*, **61**, 630, 2011.
[13] Hilal, N., Injrou, S., Karroum, R., *Arabian Journal of Mathematics*, **9**, 367, 2020.
[14] Inan, B., Osman, M.S., Ak, T., Baleanu, D., *Mathematical Methods in the Applied Sciences*, **43**, 2588, 2020.
[15] Zahra, W.K., Ouf, W.A., L-Azab, M.S., *Electronic Journal of Mathematical Analysis and Applications*, **2**(2), 81, 2014.
[16] Pathak, M., Bhatia, R., Joshi, P., Mittal, R.C., *Mathematics and Statistics*, **12**(3), 270, 2024.
[17] Nourazar, S.S., Soori, M., Nazari-Golshan, A., *Australian Journal of Basic and Applied Sciences*, **5**(8), 1400, 2011.
[18] Prakash, A., Kumar, M., *Journal of Applied Analysis and Computation*, **6**(3), 738, 2016.
[19] Li, Q., Zheng, Z., Wang, S., Liu, J., *Neural Network Advances*, **7367**, 140, 2012.
[20] Malik, A., Chand, F., Kumar, H., Mishra, S.C., *Pramana Journal of Physics*, **78**(4), 513, 2012.
[21] Akinlabi, G.O., Edeki, S.O., *Statistics Theory, arXiv*:1703.06745, 2017.
[22] Soori, M., Nourazar, S., Nazari-Golshan, A., *Advances in Theoretical and Mathematical Physics*, **5**(1), 17, 2016.
[23] Gupta, S., Goyalı, M., Prakash A., *TWMS Journal of Applied and Engineering Mathematics*, **10**(2), 312, 2020.
[24] Kumar, H., Yadav, N., *Fourth Congress on Intelligent Systems, Conference paper*, **865**, 405, 2024.
[25] Mahgoub, M.M.A., *Advances in Theoretical and Applied Mathematics*, **11**, 399, 2016.
[26] Mahgoub, M.M.A., Sedeeg, A.K.H., *American Journal of Mathematical and Computer Modelling*, **1**, 21, 2016.
[27] Hariharan, G., *Journal of Membrane Biology*, **247**, 371, 2014.

[28] Bates, P.W., Brown, S., Han, J., *International Journal of Numerical Analysis and Modeling*, **6**, 33, 2009.
[29] Hariharan, G., Kannan, K., *Applied Mathematical Sciences*, **3**, 2523, 2009.
[30] Zahra, W.K., *Mediterranean Journal of Mathematics*, **14**, 1, 2017.
[31] Ali, K.K., Mehanna, M. S., Mohamed, M. S., *Optical and Quantum Electronics*, **55**, 1, 2023.
[32] Hong, B., *Frontiers in Physics*, **10**, 1, 2022.
[33] Karakoc, S.B.G., Saha, A., Sucu, D.Y., *Mathematics and Computers in Simulation*, **203**, 12, 2023.
[34] Ali, K.K., Sucu, D. Y., Karakoc, S.B.G., *Mathematics and Computers in Simulation*, **220**, 192, 2024.
[35] Karakoc, S.B.G., Ali, K.K., Sucu, D.Y., *Journal of Computational and Applied Mathematics*, **421**, 114850, 2023.
[36] Kutluay, S., Yagmurlu, N.M., Karakaş, A. S., *Journal of Mathematical Sciences and Modelling*, **7**(2), 82, 2024.
[37] Kutluay, S., Yagmurlu, N.M., Karakaş, A.S., *Wave Motion*, **129**, 103342, 2024.
[38] Sagar, B., Ray, S.S., *Computational and Applied Mathematics*, **40**, 1, 2021.